

A highly efficient dispersant from black liquor for carbendazim suspension concentrate: Preparation, self-assembly behavior and investigation of dispersion mechanism

Nanlong Hong,^{1,2} Yuan Li,^{1,2} Xueqing Qiu^{1,2}

¹School of Chemistry and Chemical Engineering, South China University of Technology, Guangzhou, China

²State Key Laboratory of Pulp and Paper Engineering, South China University of Technology, Guangzhou, China

Correspondence to: Y. Li (E-mail: celiy@scut.edu.cn) and X. Qiu (E-mail: xueqingqiu66@163.com)

ABSTRACT: Compared with traditional approaches using synthetic amphiphilic block copolymers, alkyl chain cross-linked liginosulfonate (ASL) with high molecular weight (Mw) from black liquor was synthesized and characterized by GPC, functional group content, FTIR, and ¹H-NMR measurement, and then used as water soluble amphiphilic biopolymer to prepare polymersomes via solution self-assembly. DLS illustrated the solution assembly behavior. The hollow nature of nanospheres was revealed by TEM. Moreover, the element analysis and XPS results revealed the hollow sphere structure with a hydrophilic core and a hydrophobic shell. It facilitated the efficient encapsulation of pesticide carbendazim into the hollow sphere via electrostatic interaction, which was investigated by SEM, TEM, elemental analysis and XPS. In our study, ASLs with different Mw from 20 kDa to 200 kDa all could exhibit the similar self-assembly behavior, which suggests that the hollow spheres and the encapsulation experiment were easily duplicated from ASL polymers without structure dependence. Furthermore, the dispersion properties of ASL in the carbendazim suspension concentrate (SC) system were also investigated, which showed that SC with ASL exhibited better dispersion property and rheological performance than that of NSF and commercial LS. Preparation and application of polymersomes via self-assembly from modified-lignin from black liquor provide a promising and effective scaffold which can be conveniently obtained from cheap and renewable bioresource. © 2015 Wiley Periodicals, Inc. *J. Appl. Polym. Sci.* **2016**, *133*, 43067.

KEYWORDS: applications; biopolymers and renewable polymers; crosslinking; self-assembly

Received 29 July 2015; accepted 16 October 2015

DOI: 10.1002/app.43067

INTRODUCTION

For decades of years, amphiphilic polymeric nano- and micro-scale materials have attracted worldwide attention.^{1–4} The nano/micro-structure-property relationship is of great fundamental importance for the design of materials with industrial application potential in encapsulation and controllable release of drug^{5,6} and pesticide.^{7,8} Generally, nanostructures or microstructures were prepared from amphiphilic block polymer via template synthesis^{9,10} or emulsion polymerization.^{11,12} However, biopolymers, including proteins, nucleic acids, viruses, lipid, glucose, chitosan, lignin, cellulose, and hemicellulose, and so on,^{13–17} have attracted great attention for their biocompatibility and biodegradability. Biopolymers have emerged as an ideal candidate in the formation of nano-/micro- materials via self-assembly because of their safety, environment impact and low cost.^{13–19} Lignin, a natural biopolymer, has stimulated great fundamental interest and has widespread applications in many fields because of its advantages such as low environmental impact,

abundant in source and lower cost.^{20–29} As one of the most abundant plant biopolymers^{30–32}; however, lignin suffers from its disadvantages such as poor solubility and relatively low molecular weight (M_w) which limit its application.³³ Numerous studies have been focused on lignin to convert it into liginosulfonate (LS) by various technologies to overcome these obstacles in order to increase its application value in industrial fields.^{34–37} On the other hand, high-valued and novel utilization for modified lignin-based polymers are promoted to develop. Preparation and application of modified lignin-based nanostructures provide a promising and effective scaffold for efficient utilization of black liquor from cheap and renewable bioresource.^{18,39–41}

Recently, new progress has been made in the self-assembly and application of lignin and LS as reported previously in our lab.^{38–41} The structure-amphiphilic property relationship of LS-based molecules such as aggregation behavior in water has been studied, which abstracted great fundamental and industrial interest in biomass utilization.³⁸ Moreover, our recent research

demonstrated ACL (acetylated lignin) can fabricate uniform solid nanospheres in water/THF solution.^{39,40} More recently, CO₂-responsive diethylaminoethyl-modified lignin nanoparticles were also obtained and used as surfactant for pickering emulsion.⁴¹ However, as far as we know, hollow spheres obtained from LS via self-assembly have been rarely reported because the study on it is challenging due to their extremely complex three-dimensional amorphous structure.

Herein, for the aim of improving the amphiphilicity of lignin to obtain hollow spheres, we describe a modification of lignin using black liquor as starting material to prepare alkyl chain assisted lignosulfonate polymer (ASL).¹⁸ In previous article, lignosulfonate (LS) was directly used to be modified and then used to disperse coal-water slurry. However, black liquor was directly used to be sulfonated and cross-linked in this work. The cost of the product is far lower than that of the previous work. The chemical structure of SL is very different from that of LS (see Figure 3), because the sulfonation approaches between them are very different. LS was obtained by sulfonation with Na₂SO₃ at high pressure and temperature, however, SL was obtained by sulfonation with CH₂O and Na₂SO₃ at atmospheric pressure and relatively low temperature. Another novelty of this work is encapsulation of pesticide carbendazim using hollow spheres. The reaction steps of ASL is as follows: sulfomethylation of black liquor as raw material followed by further polymerization between sulfomethylated lignin (SL) and 1,6-dibromohexane. For our approach, the introduction of alkyl chain into SL molecules was an easily accessible hydrophobic modification route to improve M_w of lignin, and the further polymerized SLs via alkyl chain bridging were rarely reported, to date. The modified lignin-based polymer ASLs with different M_w from 20 kDa to 200 kDa could self-assemble into polymersomes in selective solvents. In this work, ASL with moderate M_w was utilized as a representative product to investigate the self-assembly behavior. The result is an interesting observation unreported previously. As previously mentioned, Wang *et al.*⁸ utilized layer-by-layer self-assembly method to encapsulate the herbicide picloram, which was relatively sophisticated to operate. Carbendazim, a representative benzimidazolic compound, has been also widely used as a pesticide and herbicide for the protection of plant.⁴² In our work, pesticide carbendazim was encapsulated into ASL hollow spheres during the ASL self-assembly process by electrostatic interaction, which was investigated by SEM, TEM, elemental analysis and XPS. Furthermore, the carbendazim suspension concentrate (SC) with ASL dispersant exhibited better dispersion properties than that of NSF and commercial LS.

MATERIALS AND METHOD

Materials

Lignin black liquor was supplied by Shuntai (Shuntai, Hunan, China). 1,6-dibromohexane (C₆H₁₂Br₂) was supplied by Energy Chemical (Shanghai, China) with a purity of 97%. All other chemicals were of analytical grade, including formaldehyde (CH₂O) of 37%, sodium hydroxide (NaOH), sodium sulfite (Na₂SO₃), potassium iodide (KI), hexane, ethanol (EtOH) and pesticide carbendazim. The commercial LS product was sup-

plied by Shixian Paper Mill (Jilin Province, China). NSF (naphthalene sulfonate-formaldehyde condensate) was a commercial dispersant of Zhanjiang additive company (Guangdong, China).

Preparation of ASL

Black liquor (10 g) was dissolved in 50 mL of H₂O at pH of 12. The reaction was started by slow addition of formaldehyde (2.1 g) at 70°C for 20 min, and subsequent addition of sodium sulfite (4.0 g) at 95°C. After the reaction was kept for 3 h, the reaction liquid was added C₆H₁₂Br₂ (2.5 g), 5.0 g of NaOH and trace amount of KI (0.1 g) at 80°C, respectively. The polymerization was stopped after reflux at 80°C for 8 h. The sample was then extracted with hexane to remove the excessive C₆H₁₂Br₂ and the polymer in aqueous solution was filtered. The filtrates were purified with dialysis ($M_w = 1000$ Da) to removed inorganic salt. The purified product was then freeze-dried to obtain yellow-brown solid powder sample.

Gel Permeation Chromatography (GPC) Measurement

Calibration standard was polystyrene sulfonate with M_w range from 2 to 150 kDa. The eluent was 0.10M NaNO₃ solution of 0.50 mL/min. All samples were dissolved and diluted into 0.3 wt % using double-distilled water and filtered by a 0.22- μ m filter. The M_w measurement was conducted by aqueous gel permeation chromatography and the UV absorption at 280 nm was monitored with a Waters 2487 UV detector (Waters Co, Milford, MA).

Functional Group Content Measurement

The phenolic hydroxyl group (-OH) content of samples was determined by Folin-Ciocalteu colorimetric (FC) method. The sulfonic group (-SO₃H) content of SL and ASLs was measured by automatic potentiometric titrator (Type 809 Titrando. Metrohm Corp., Switzerland).

Infrared Spectroscopy Analysis

FTIR spectra of SL and ASL were measured on an AutosystemXL/I-series/Spectrum2000 (Thermo Nicolet Co., Madison, WI) and recorded between 4000 and 400 cm⁻¹. The measurement method was potassium bromide pressed-disk technique.

¹H-NMR Spectroscopy Analysis

The ¹H-NMR spectra of samples were recorded with 30 mg of each sample dissolved in 0.5 mL of deuterium oxide (D₂O) at room temperature by DRX-400 spectrometer (Bruker Co., Ettlingen, Germany).

Preparation of Polymersome with ASL

First, ASL was dissolved into water to prepare ASL solution (0.5 mg/mL), and then ethanol was added into the ASL aqueous solution to achieve a solution of 0.05 mg/mL. Then, the mixed solution was stirred for around 3 h and left for 1 h at room temperature to obtain the ASL polymersomes.

Scanning Electron Microscopy (SEM)

Scanning electron micrographs were recorded with a Nova Nano SEM instrument (Zeiss, Netherlands). Samples were mounted on aluminum stubs by means of double-sided conductive adhesive and sputtered with Au/Pd to reduce charging effects. The concentration of samples was 0.05 mg/mL, and the

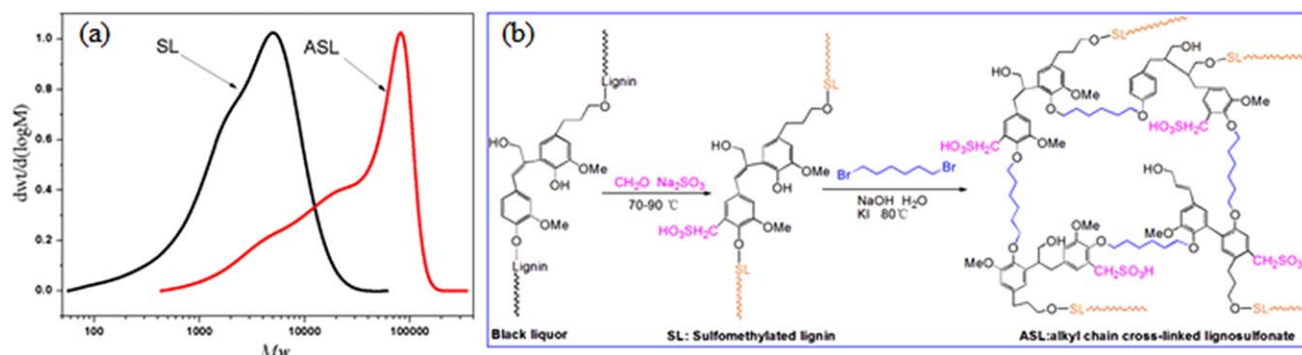


Figure 1. (a) Effect of 1,6-dibromohexane (C₆H₁₂Br₂) on molecular weight distribution of ASL. (b) The reaction scheme of ASL from black liquor. [Color figure can be viewed in the online issue, which is available at wileyonlinelibrary.com.]

volume proportion of solvents was 1:9 which were water and ethanol.

Transmission Electron Microscopy (TEM)

The TEM samples were prepared by dropping diluted sample solution onto the copper grids coated with a thin carbon film. The concentration of samples was 0.05 mg/mL in H₂O/Ethanol (v/v, 1:9). TEM images were obtained using a HITACHI H-7650 electron microscope with an accelerating voltage of 200 kV.

Dynamic Light Scattering (DLS) Measurement

Experiments were performed on Zeta PALS instrument (Brookhaver, USA). The concentration of samples was 0.05 mg/mL in H₂O/Ethanol (v/v, 1/9).

Element Content Measurement

Elemental analyses of SL and ASL were measured by Elementar Vario EL cube. Elemental distribution on the surface of ASL particles was analyzed by X-ray photoelectron spectroscopy (XPS, Ultra Axis DLD, Kratos, England). The nanosphere samples for XPS were prepared by dropping the TEM samples solution on tinfoil and drying naturally under room temperature. The bulk materials were obtained by freeze-drying and analyzed. Elemental distribution of the colloidal spheres loading of pesticide carbendazim was also determined by elemental analysis and XPS.

Encapsulation of Pesticide Carbendazim

The carbendazim was first dissolved into HCl aqueous solution (0.1 mol/L) to prepare 5 mg/mL. 0.58 mL of carbendazim solution was mixed with 90 mL of EtOH. The solution was added into 10 mL of 0.5 mg/mL ASL aqueous solution and the H₂O/EtOH mixed sample solution was stirred for 3 h at room tem-

perature. The encapsulation of pesticide was proceed during nanocapsules formation, and the ratio of n(carbendazim): n(-SO₃H) was 1.5:1. The mixed sample solution was dialyzed to remove excess carbendazim. The result of encapsulation was observed by SEM, TEM, and elemental analyses.

Preparation of Carbendazim Suspension Concentrates (SC)

In this work, 45% carbendazim SC were prepared by wet milling with a planetary ball mill (QM-3SP2, Nanjing University Instrument Factory, China). Carbendazim (45 g), dispersant (3 g), and Milli-Q water (52 g) were mixed and added to a grinding jar filled with zirconium balls (300 g) with a diameter of 10 mm. The rotation rate was set at 400 r/min and ran for 2 h to target particle size <5 μm, thus carbendazim SC with different dispersants were obtained.

Dispersion Properties in Carbendazim SC And Rheological Property Measurements

Suspensibility tests of carbendazim SC were conducted according to Collaborative International Pesticides Analytical Council (CIPAC) Method MT161. The remaining tenth of the suspension was assayed gravimetrically after it was dried, and the total suspensibility was calculated. Each sample was measured in triplicate.

Rheological properties of carbendazim SC with different dispersants were performed employing a rheometer (Haake MARS III). The shear rate range is: up run 0~200 s⁻¹ and the temperature is kept at 25°C, with a fluctuation of 1°C. Shear stress and shear viscosity were monitored, and the viscosity at shear rate of 100 s⁻¹ was used as the apparent viscosity of carbendazim SC.

Table I. Effect of 1, 6-dibromohexane (C₆H₁₂Br₂) on the Molecular Weight Distributions and Functional Group Contents of Alkyl Chain Cross-Linked Liginosulfonate (ASL)

Samples	m (black liquor): m (C ₆ H ₁₂ Br ₂)	M _w (Da)	M _n (Da)	PDI	Functional group contents	
					-OH (mmol/g)	-SO ₃ H (mmol/g)
SL	1:0.00	4450	1,550	2.87	2.23	1.79
ASL	1:0.25	55,800	17,900	3.12	0.45	1.64

SL, sulfomethylated lignin; PDI, polydispersity index.

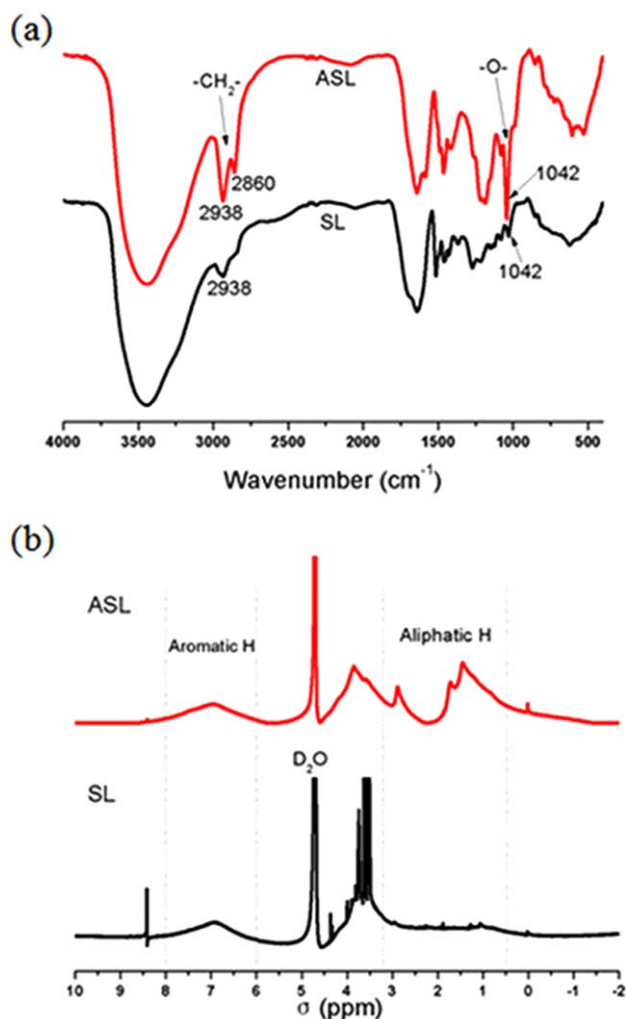


Figure 2. FTIR spectra (a) and $^1\text{H-NMR}$ spectra (b) of SL and ASL polymer. [Color figure can be viewed in the online issue, which is available at wileyonlinelibrary.com.]

RESULTS AND DISCUSSIONS

Measurements of Molecular Weight Distribution

As can be seen from Figure 1(a), alkyl chain assisted LS-based polymer ASL with high molecular weight was prepared by our designed reaction. The effect of $\text{C}_6\text{H}_{12}\text{Br}_2$ on the molecular

Table II. FTIR Bands Assignment of ASL Polymer

Band (cm^{-1})	Vibration	Assignment
3,450–3,405	st O–H	Phenolic OH and aliphatic OH
2,950–2,920	st C–H	CH_3 and CH_2
2,860	st C–H	OCH_3
1,650	st C=O	Conjugated C=O
1,600	st C–C	Aromatic skeleton
1,500	st C–C	Aromatic skeleton
1,410	st C–C	Aromatic skeleton
1,042	st C–O(C)	Ether –O–

st, stretching vibration.

Table III. Signal Assignment for $^1\text{H-NMR}$ Spectrometry of ASL Polymer

Signal (ppm)	Assignment
8.0–6.0	Aromatic H in S and G units
6.9	Aromatic H in G
6.6	Aromatic H in S
3.7–4.0	Methoxyl H
3.0–0.5	Aliphatic H

weight of ASL was obvious. The results of M_w distribution were also listed in Table I, the M_w of ASL ($M_w = 55,800$ Da) increased by a factor of 12-fold for SL ($M_w = 4450$ Da). ASL polymer were readily obtained by two steps in one pot: sulfomethylation of black liquor to prepare sulfomethylated lignin (SL) and further polymerization between SL and 1,6-dibromohexane in NaOH aqueous solution. Compared with the conventional modification routes, our method is easy processing and cost-efficient procedure.

Functional Group Content Analyses

In order to study the chemical structure of ASL polymer, functional groups, such as phenolic hydroxyl groups and sulfonic groups, were analyzed. As shown in Table I, after alkyl chain assisted modification, the phenolic hydroxyl group content of ASL decreased remarkably from 2.23 mmol/g to 0.45 mmol/g. This suggested a straightforward relationship between the polymerization of SL and consumption of phenolic hydroxyl groups.

The content of sulfonic groups decreased slightly after alkyl chain assisted polymerization with $\text{C}_6\text{H}_{12}\text{Br}_2$ as shown in Table I. The results can be explained by the increase of M_w due to the increasing introduction amount of alkyl chains. The sulfonic group content of SL was 1.79 mmol/g, the total amount of sulfonic groups could be unchanged by alkyl chain cross-linked polymerization, so the sulfonic group contents decreased slightly after increasing M_w of SL. The results were verified by elemental analysis shown in Table IV. The content of SL and ASL is 5.67% and 5.32%, respectively, which could be converted to 1.78 mmol/g and 1.66 mmol/g for SL and ASL. Therefore, the result detected by elemental analysis was very close to that detected by automatic potentiometric titration.

Chemical Characterization

To elucidate the chemical structure of ASL polymer, the FTIR spectra of SL and ASL were investigated as shown in Figure

Table IV. Elemental Distribution of SL and ASL Bulk Materials by Elemental Analysis Method (left), and ASL Nanosphere on Its Surface by XPS Method (Right)

Samples	Elemental analysis			XPS method			Br %
	C %	S %	C/S	C %	S %	C/S	
SL	31.07	5.67	5.48	-	-	-	-
ASL	48.96	5.32	9.20	73.96	2.69	27.49	-

–, means none of detection.

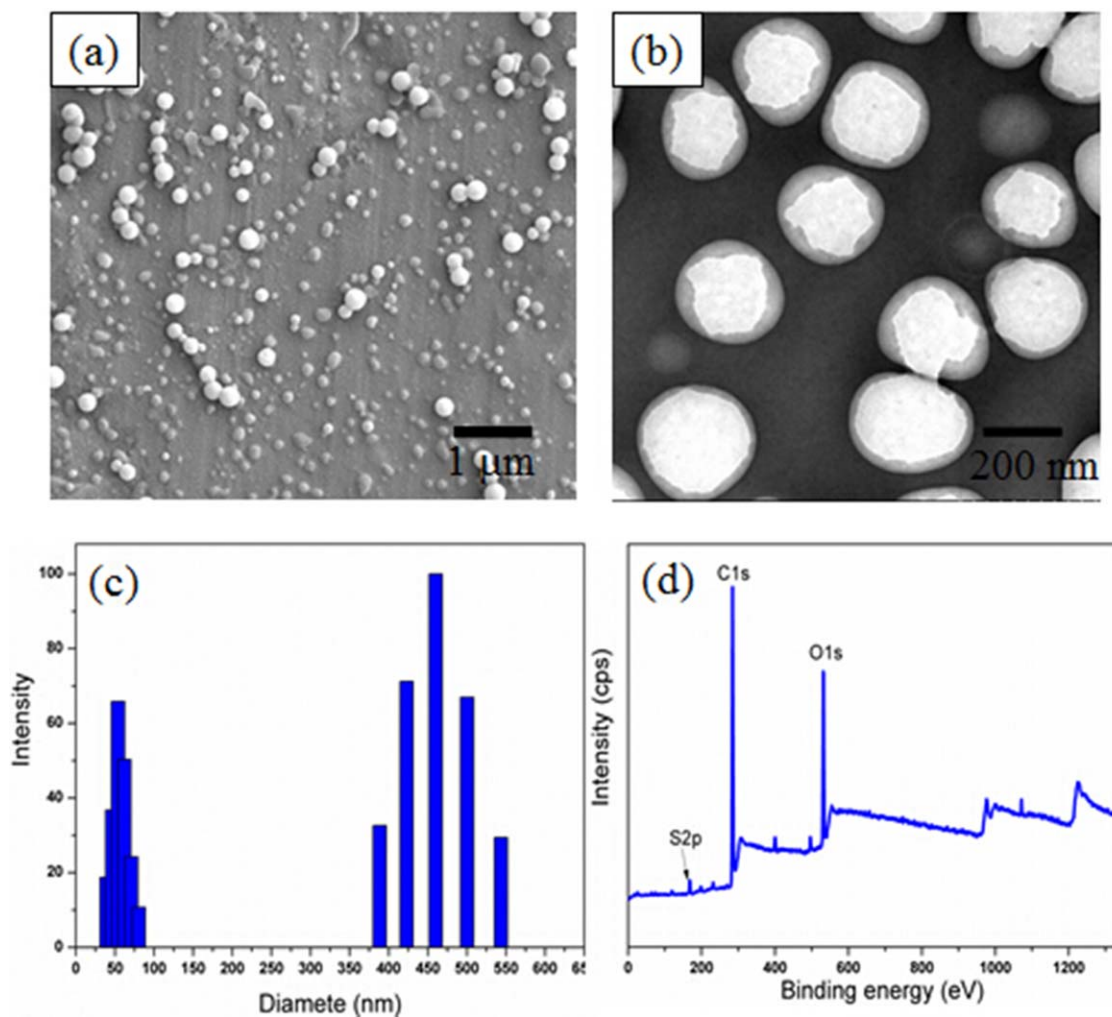


Figure 3. Surface morphology of the polymersomes obtained from ASL suspension: SEM image (a) and TEM image (b). Particle size distribution (c) and XPS (d) of ASL polymersomes via self-assembly in selective solvent. [Color figure can be viewed in the online issue, which is available at wileyonlinelibrary.com.]

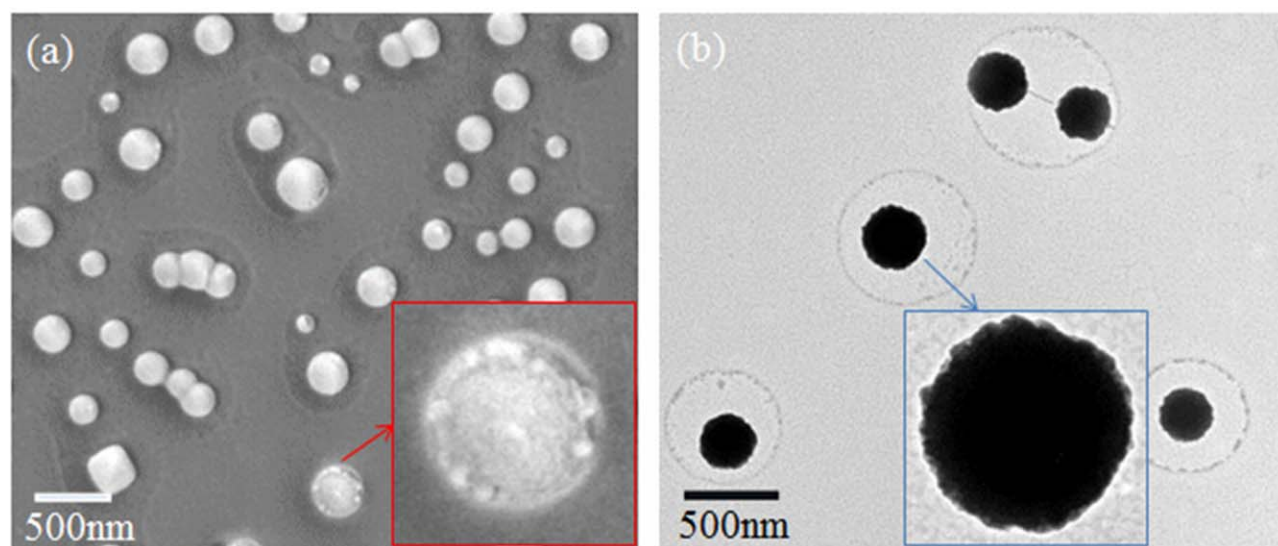


Figure 4. SEM image (a) and TEM image (b) of ASL polymersomes encapsulated of pesticide carbendazim. [Color figure can be viewed in the online issue, which is available at wileyonlinelibrary.com.]

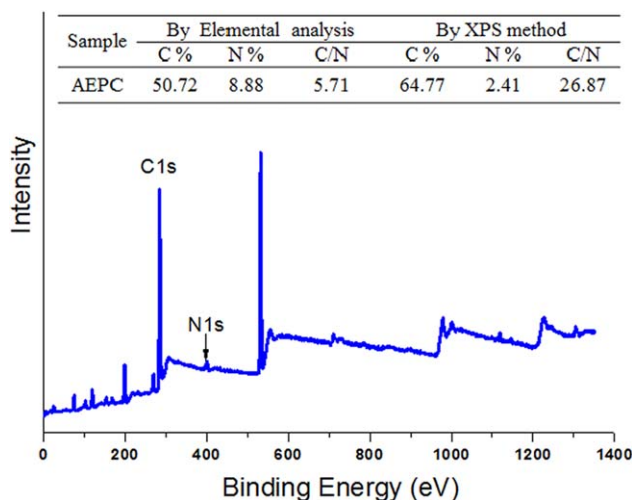


Figure 5. Elemental distributions of ASL polymersomes encapsulated of pesticide carbendazim (AEPC) (table inserted in the figure was elemental distribution of the colloidal spheres detected by elemental analysis and XPS). [Color figure can be viewed in the online issue, which is available at wileyonlinelibrary.com.]

2(a), and the FTIR bands assignment was listed in Table II. The intensity of band from 3450 to 3405 cm^{-1} corresponding to phenolic group stretching vibrations decreased significantly, which was in accordance with the results concerning phenolic groups content (Table I). It also further indicated that the reaction sites are phenolic hydroxyl groups and $\text{C}_6\text{H}_{12}\text{Br}_2$ was reacted with $-\text{OH}$ of SL to prepare ASL. The areas of bands at 2938 cm^{-1} and 2860 cm^{-1} corresponded to methylene stretching vibrations from alkyl chain. The area at 1042 cm^{-1} corresponded to ether bond stretching vibration. The intensities of A_{2938} , A_{2860} , and A_{1042} all increased as a result of efficient substitutions of aliphatic chains on phenolic groups of SL.

For the in-depth elucidation of structural features of ASL polymer, SL and ASL were also subjected to $^1\text{H-NMR}$ analysis [Figure 2(b)]. The signal assignment for $^1\text{H-NMR}$ spectra of ASL is also listed in Table III. As shown in Figure 2(b) and Table III, after alkyl chain assisted polymerization, the signal intensity below 3.0 ppm exhibited significant increase which was ascribed to aliphatic chain $-\text{C}_6\text{H}_{12}-$ groups and was in good agreement with the IR results. The signal intensity of aromatic protons at 8.0–6.0 ppm exhibited no observable change between SL and ASLs. Moreover, X-ray photoelectron spectroscopy (XPS) of ASL nanospheres [Table IV and Figure 3(d)] was also conducted to test the content of bromine element, but none of Br was detected in ASL sample. If the SL molecules were connected linearly by $-\text{C}_6\text{H}_{12}-$ groups, under excessive addition of $\text{C}_6\text{H}_{12}\text{Br}_2$,

the $-\text{C}_6\text{H}_{12}\text{Br}$ groups should be detected by XPS. The GPC [Figure 1(a) and Table I], IR, $^1\text{H-NMR}$, and XPS results demonstrated that both the intermolecular and intramolecular nucleophilic substitution reactions between $\text{C}_6\text{H}_{12}\text{Br}_2$ and SL molecules simultaneously occurred efficiently. As a result, the cross-linked network structure of amphiphilic polymer ASL was proposed to be produced during the polymerization reaction as shown in Figure 1(b). Our key concept for polymer design is that sulfonation and polymerization occur on the ortho-positions and $-\text{OH}$ positions of phenol hydroxyl groups, respectively, which avoid the two simultaneously competitive reactions on the ortho-positions of phenol hydroxyl groups.

Preparation of ASL Polymersomes via Self-Assembly

ASL, obtained from alkyl chain-assisted polymerization of SL, was used as an amphiphilic biopolymer to fabricate polymersomes via self-assembly behavior. The critical influences of the self-assembly behavior include hydrophilic-hydrophobic property of polymer, the proportion of mixed solvent, stirring speed and stirring time. In our study, we used the optimal condition to prepare ASL polymersome (see 2.7 of methods). As can be seen the SEM image from Figure 3(a), ASL was found to form compact nanospheres and the average diameter of the nanospheres was around 200~300 nm, which was proposed to be driven by a reduction of surface energy.^{43,44}

More importantly, TEM was performed to study the nanosphere structure from ASL polymer as shown in Figure 3(b). The result of TEM image is very similar with previous polymer-only hollow spheres.^{43,45} The middle core of spheres was apparently shallower than the periphery side, which suggested they were hollow spheres. TEM of ASL nanospheres showed the spherically shaped hollow structure [Figure 3(b)] and the diameter was also around 200~300 nm. Therefore, we propose the self-assembly model of ASL polymersomes via self-assembly behavior, as shown in Figure 7. The three-dimensional network structure of ASL polymer promotes the amphiphilic LS-polymer to form polymersomes in selective solvent by self-assembly.

DLS and Elemental Distribution Analyses of ASL Polymersomes

DLS measurement was conducted to study the assembly behavior in solution. As can be seen the particle size distribution from Figure 3(c), a small percentage of particles from 30 to 80 nm were detected in the dynamic light scattering measurement, and most of polymersomes from 370 to 550 nm existed in the solution. The particle size detected by DLS was relatively larger than that from SEM and TEM. Because the polymersomes could swell in the solution, which makes the spheres relatively larger than that detected by SEM. Therefore, we think the DLS result was in

Table V. Dispersion Properties of 45% Carbendazim SC with Different Dispersants

Samples	Dispersant dosage (%)	SC (%)	Suspensibility (%)	apparent viscosity (mPa.s)
ASL	3	46.8	96 ± 0.9	80.14
NSF	3	45.9	86 ± 1.5	296.58
Commercial LS	3	46.5	90 ± 1.1	184.93

NSF, naphthalene sulfonate-formaldehyde condensate.

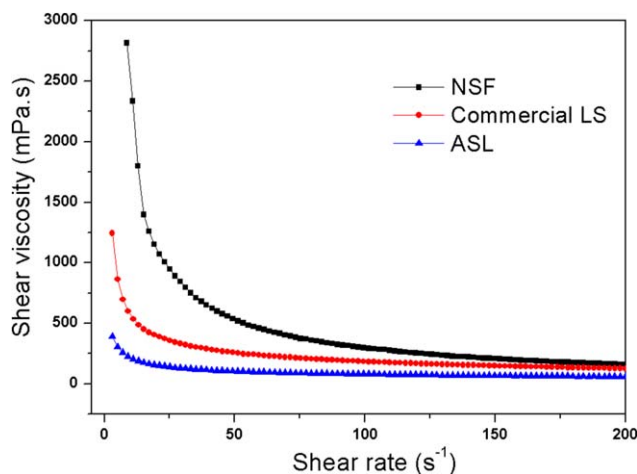


Figure 6. Shear viscosity curve of 45% carbendazim SC prepared with 3% dispersants (NSF: naphthalene sulfonate-formaldehyde condensate). [Color figure can be viewed in the online issue, which is available at wileyonlinelibrary.com.]

good accordance with the self-assembly process in solution to fabricate polymersomes detected by SEM and TEM. From this approach, nanometer-sized polymersomes can be readily prepared which is important for its further application.

The elemental distribution of SL and ASL estimated by elemental analysis and XPS method was shown in Figure 3(d) and Table IV. Element analysis was used to test the C/S element ratio of the whole sphere, and XPS was used to analyze the C/S element ratio of the surface of the polymersome. The C/S element ratio of ASL ($C/S = 9.20$) is higher than that of SL ($C/S = 5.48$) detected by element analysis, which was an important contributing factor on the self-assembly of ionic polymer.⁴⁶ More importantly, the C/S element ratio of the surface of ASL nanospheres ($C/S = 27.49$) detected by XPS is remarkably higher than those of bulk materials ($C/S = 9.20$)

detected by elemental analysis, which showed a higher content of $-SO_3H$ groups inside the polymersome. It also means that the hollow nanoparticles expose a hydrophobic surface in the mixed solution as shown in the proposed self-assembly model of Figure 7.

Encapsulation of Pesticide Carbendazim

Based on the preparation of polymersome, the core of the polymersome with a higher content of $-SO_3H$ groups makes the ASL polymersome potentially useful in many applications due to the presence of electrostatic attraction between sulfonic group and other cationic groups to achieve efficient encapsulation of guest molecules including pesticide and drug. In this work, ASL polymersomes were employed for the loading of pesticide carbendazim, which was investigated by SEM and TEM (Figure 4). The encapsulation of pesticide was obtained by adding carbendazim dissolved in HCl aqueous solution to the ASL $H_2O/EtOH$ mixed solution during polymersome formation, and the ratio of $n(\text{carbendazim}) : n(-SO_3H)$ was 1.5:1. As can be seen from Figure 4(a), SEM image of the nanospheres loading of carbendazim molecules was different from that of polymersomes. Dimly, as shown in the red arrow of Figure 4(a), we can see that the pesticide crystal was encapsulated in the polymersome. Polymersomes were changed into colloidal nanospheres due to the loading of the pesticide carbendazim as shown in Figure 4(b). The middle core of nanospheres was apparently darker than the periphery side shown in the blue arrow of Figure 4(b), which further verified the SEM result shown in Figure 4(a).

To determine the encapsulation of the pesticide carbendazim, elemental distribution of the colloidal spheres loaded of pesticide carbendazim was performed as shown in Figure 5. The C/N ratio of the whole colloidal sphere can be estimated by elemental analysis, while the C/N ratio on the surface of colloidal sphere can be observed by XPS. As shown in the Table inserted in Figure 5, the C/N ratio of the whole colloidal sphere is 5.71, but the C/N ratio on the colloidal sphere surface is 26.87. It shows a direct evidence to support that the

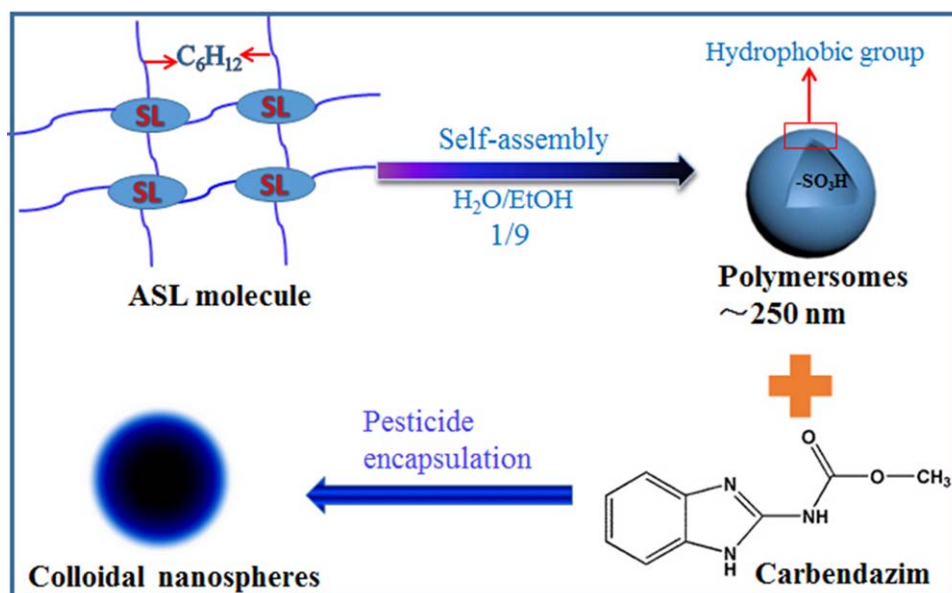


Figure 7. Self-assembly model of polymersomes and its encapsulation of pesticide carbendazim. [Color figure can be viewed in the online issue, which is available at wileyonlinelibrary.com.]

pesticide carbendazim was encapsulated inside the ASL polymer-some, which also further verified the results of SEM and TEM. Therefore, we propose the encapsulation model of pesticide carbendazim as shown in Figure 7. During the formation process of ASL polymersomes, carbendazim was added into the solution and then was encapsulated into the polymersomes via electrostatic interaction between sulfonic group of ASL and ammonium of carbendazim.

Evaluation of ASL Used for Carbendazim SC Preparation

In the research results previously, pesticide carbendazim was encapsulated into the ASL polymersomes efficiently. Therefore, the carbendazim SC prepared with ASL was also evaluated in our work. The dispersion properties of 45% carbendazim SC with different dispersants were investigated including suspensibility and apparent viscosity as shown in Table V and Figure 6. When preparing 45% carbendazim SC with 3% dispersant including ASL, naphthalene sulfonate-formaldehyde condensate (NSF) and commercial LS, it was found that carbendazim SC with ASL exhibited better fluidity than that of NSF and commercial LS. The shear viscosity of carbendazim SC prepared with ASL is remarkably lower than that of NSF and commercial LS as shown in Figure 6. The viscosity at shear rate of 100 s^{-1} was used as the apparent viscosity of carbendazim SC, which was 80.14, 296.58, and 184.93 mPa.s corresponding to dispersant ASL, NSF and commercial LS, respectively (Table V). As can be seen from Table V, the suspensibility of carbendazim SC prepared with above dispersants was 96%, 86%, and 90% corresponding to ASL, NSF, and commercial LS, respectively. The results indicated that ASL exhibited better dispersion performance for carbendazim SC than NSF and commercial LS.

CONCLUSIONS

In conclusion, ASL polymer with high M_w was readily prepared by alkyl chain assisted polymerization using black liquor as raw materials by two steps in one pot. Polymersomes were easily prepared via self-assembly of water soluble ASL polymer with such complex three-dimensional amorphous structure. The formation mechanism was preliminary studied by SEM, TEM, and DLS. The hydrophobic alkyl chain blocks contribute to the self-assembly which make it easily achievable to rearrange and fabricate hollow sphere structure which was investigated by XPS and TEM. Moreover, nanocapsules were utilized to encapsulate pesticide carbendazim effectively via electrostatic interaction between sulfonic group of ASL and ammonium of carbendazim, it was investigated by SEM, TEM, elemental analysis and XPS. Furthermore, ASL exhibited better dispersion performance for carbendazim SC than NSF and commercial LS. This work provides new design concept and synthetic approach for LS-based polymers with easily accessible self-assembly with potential applications such as microencapsulation. Our self-assembly systems based on lignosulfonate showed obvious advantages over the existing ones reported in literatures and may provide a promising and effective scaffold for further development of the green industrial materials with great application potential including targeted drug delivery, microencapsulation of pesticides for controlling release, and biomedical imaging.

ACKNOWLEDGMENTS

The authors would like to acknowledge the financial support of National Basic Research Program of China 973 (2012CB215302),

International S&T Cooperation Program of China (2013DFA41670), National Natural Science Foundation of China (21436004, 21402054, 21476092, 21404043).

REFERENCES

1. Kim, H. J.; Kim, T.; Lee, M. *Accounts Chem. Res.* **2011**, *44*, 72.
2. Jain, S.; Bates, F. S. *Science* **2003**, *300*, 460.
3. Zheng, R. H.; Liu, G. J.; Yan, X. H. *J. Am. Chem. Soc.* **2005**, *127*, 15358.
4. Mane, S. R.; Shunmugam, R. *ACS Macro Lett.* **2014**, *3*, 44.
5. Lavasanifar, A.; Samuel, J.; Kwon, G. S. *Adv. Drug Deliver. Rev.* **2002**, *54*, 169.
6. Wang, K.; Liu, Y.; Li, C.; Cheng, S. X.; Zhuo, R. X.; Zhang, X. Z. *ACS Macro Lett.* **2013**, *2*, 201.
7. Kulkarni, A. R.; Soppimath, K. S.; Aminabhavi, T. M.; Dave, A. M.; Mehta, M. H. *J. Control. Release* **2000**, *63*, 97.
8. Wang, X. J.; Zhao, J. *J. Agr. Food Chem.* **2013**, *61*, 3789.
9. Choi, W. S.; Park, J. H.; Koo, H. Y.; Kim, J. Y.; Cho, B. K.; Kim, D. Y. *Angew. Chem. Int. Ed. Engl.* **2005**, *44*, 1096.
10. Watson, S. M. D.; Galindo, M. A.; Horrocks, B. R.; Houlton, A. *J. Am. Chem. Soc.* **2014**, *136*, 6649.
11. Groison, E.; Brusseau, S.; D'Agosto, F.; Magnet, S.; Inoubli, R.; Couvreur, L.; Charleux, B. *ACS Macro Lett.* **2012**, *1*, 47.
12. Lu, F. J.; Luo, Y. W.; Li, B. G.; Zhao, Q.; Schork, F. J. *Macromolecules* **2010**, *43*, 568.
13. Yin, P.; Choi, H. M. T.; Calvert, C. R.; Pierce, N. A. *Nature* **2008**, *451*, 318. U4.
14. Koltover, I. *Nat. Mater.* **2004**, *3*, 584.
15. Wang, J. *ChemPhysChem* **2009**, *10*, 1748.
16. Wang, Y. J.; Wang, J.; Ge, L.; Liu, Q.; Jiang, L. Q.; Zhu, J. B.; Zhou, J. P.; Xiong, F. *J. Appl. Polym. Sci.* **2013**, *127*, 3749.
17. Baker, D. A.; Rials, T. G. *J. Appl. Polym. Sci.* **2015**, *130*, 713.
18. Hong, N. L.; Li, Y.; Zeng, W. M.; Zhang, M. K.; Peng, X. W.; Qiu, X. Q. *RSC Adv.* **2015**, *5*, 21588.
19. Hong, N. L.; Qiu, X. Q.; Deng, W. Y.; He, Z. C.; Li, Y. *RSC Adv.* **2015**, *5*, 90913.
20. Lora, J. H.; Glasser, W. G. *J. Polym. Environ.* **2002**, *10*, 39.
21. Kumar, M. N. S.; Mohanty, A. K.; Erickson, L.; Misra, M. J. *Biobased. Mater. Bio* **2009**, *3*, 1.
22. Mialon, L.; Pemba, A. G.; Miller, S. A. *Green Chem.* **2010**, *12*, 1704.
23. Saidane, D.; Barbe, J. C.; Birot, M.; Deleuze, H. *J. Appl. Polym. Sci.* **2010**, *116*, 1184.
24. Vishtal, A.; Kraslawski, A. *Bioresources* **2011**, *6*, 3547.
25. Auvergne, R.; Caillol, S.; David, G.; Boutevin, B.; Pascault, J. P. *Chem. Rev.* **2014**, *114*, 1082.
26. Thielemans, W.; Can, E.; Morye, S. S.; Wool, R. P. *J. Appl. Polym. Sci.* **2015**, *83*, 323.
27. Teng, N. Y.; Dallmeyer, I.; Kadla, J. F. *Ind. Eng. Chem. Res.* **2013**, *52*, 6311.

28. Li, Y.; Hong, N. L. *J. Mater. Chem. A* **2015**, *3*, 21537.
29. Ten, E.; Vermerris, W. *J. Appl. Polym. Sci.* **2015**, *132*, DOI: 10.1002/app.42069.
30. Boerjan, W.; Ralph, J.; Baucher, M. *Annu. Rev. Plant Biol.* **2003**, *54*, 519.
31. Vanholme, R.; Morreel, K.; Ralph, J.; Boerjan, W. *Curr. Opin. Plant Biol.* **2008**, *11*, 278.
32. Jex, C. N.; Pate, G. H.; Blyth, A. J.; Spencer, R. G. M.; Hernes, P. J.; Khan, S. J.; Baker, A. *Quaternary Sci. Rev.* **2014**, *87*, 46.
33. Kubo, S.; Kadla, J. *Biomacromolecules* **2005**, *6*, 2815.
34. Sun, Y.; Qiu, X. Q.; Liu, Y. Q. *Biomass Bioenergy* **2013**, *55*, 198.
35. Gouveia, S.; Fernández-Costas, C.; Sanromán, M. A.; Moldes, D. *Bioresour. Technol.* **2012**, *121*, 131.
36. Qiu, X. Q.; Zeng, W. M.; Yu, W.; Xue, Y. Y.; Pang, Y. X.; Li, X. Y.; Li, Y. *ACS Sustain. Chem. Eng.* **2015**, *3*, 1551.
37. Hong, N. L.; Yu, W.; Xue, Y. Y.; Zeng, W. M.; Huang, J. H.; Xie, W. Q.; Qiu, X. Q.; Li, Y. *Holzforschung* **2015**, DOI: 10.1515/hf-2015-0043.
38. Qiu, X. Q.; Kong, Q.; Zhou, M. S.; Yang, D. J. *J. Phys. Chem. B.* **2010**, *114*, 15857.
39. Qian, Y.; Deng, Y. H.; Qiu, X. Q.; Li, H.; Yang, D. J. *Green Chem.* **2014**, *16*, 2156.
40. Qian, Y.; Deng, Y. H.; Li, H.; Qiu, X. Q. *Ind. Eng. Chem. Res.* **2014**, *53*, 10024.
41. Qian, Y.; Zhang, Q.; Qiu, X. Q.; Zhu, S. P. *Green Chem.* **2014**, *16*, 4963.
42. Jia, L.; Wong, H.; Wang, Y.; Garza, M.; Weitman, S. D. *J. Pharm. Sci.* **2003**, *92*, 161.
43. Kim, D.; Kim, E.; Kim, J.; Park, K. M.; Baek, K.; Jung, M.; Ko, Y. H.; Sung, W.; Kim, H. S.; Suh, J. H.; Patk, C. G.; Na, O. S.; Lee, D. K.; Lee, K. E.; Han, S. S.; Kim, K. *Angew. Chem. Int. Ed. Engl.* **2007**, *46*, 3471.
44. Zhou, T. Y.; Lin, F.; Li, Z. T.; Zhao, X. *Macromolecules* **2013**, *46*, 7745.
45. Sunintaboon, P.; Ho, K. M.; Li, P.; Cheng, S. Z. D.; Harris, F. W. *J. Am. Chem. Soc.* **2006**, *128*, 2168.
46. Akiyoshi, K.; Kang, E. C.; Kurumada, S.; Sunamoto, J.; Principi, T.; Winnik, F. M. *Macromolecules* **2000**, *33*, 3244.